Evaluation of a long axial field-of-view PET scanner for non-human primates

E. Berg, X. Zhang, J. Bec, M.S. Judenhofer, Q. Peng, M. Kapusta, M. Schmand, M.E. Casey, J. Qi, R.D. Badawi and S.R. Cherry

eberg@ucdavis.edu

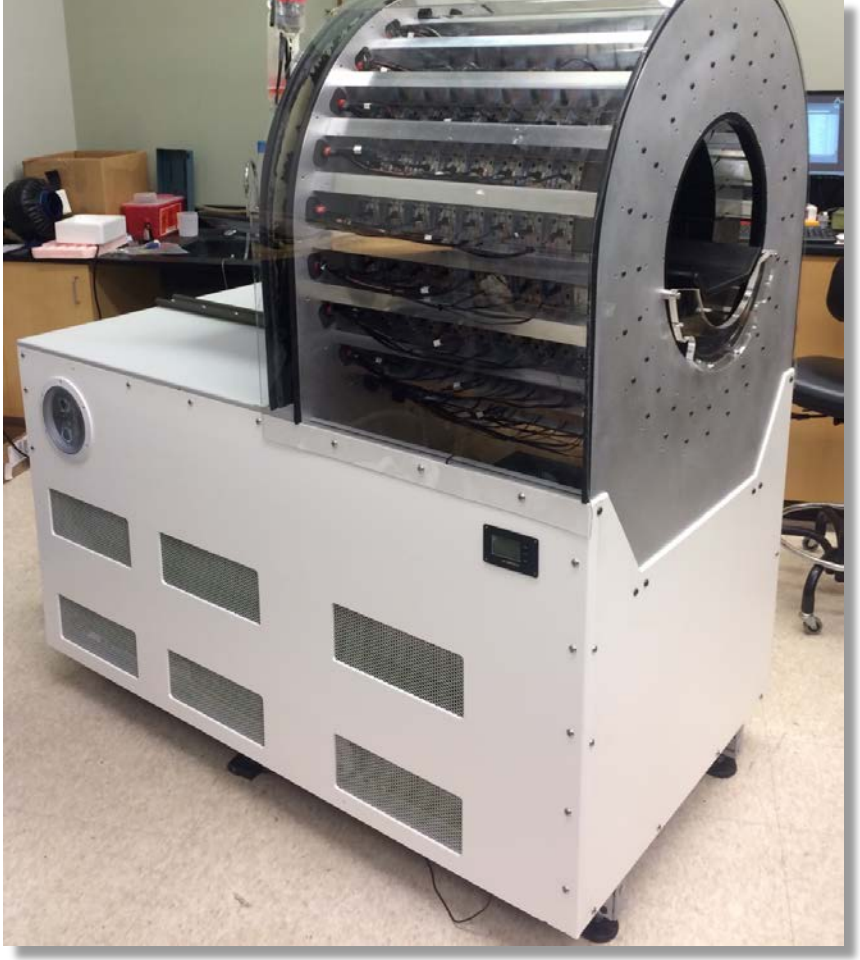

mini-EXPLORER: a long axial field-of-view PET scanner for monkey imaging

- Support PET imaging studies at the California National Primate Research Center (CNPRC)
  - Stem cells
  - Viral sanctuaries

- Investigate changes in scanner performance and image quality with a wide acceptance angle

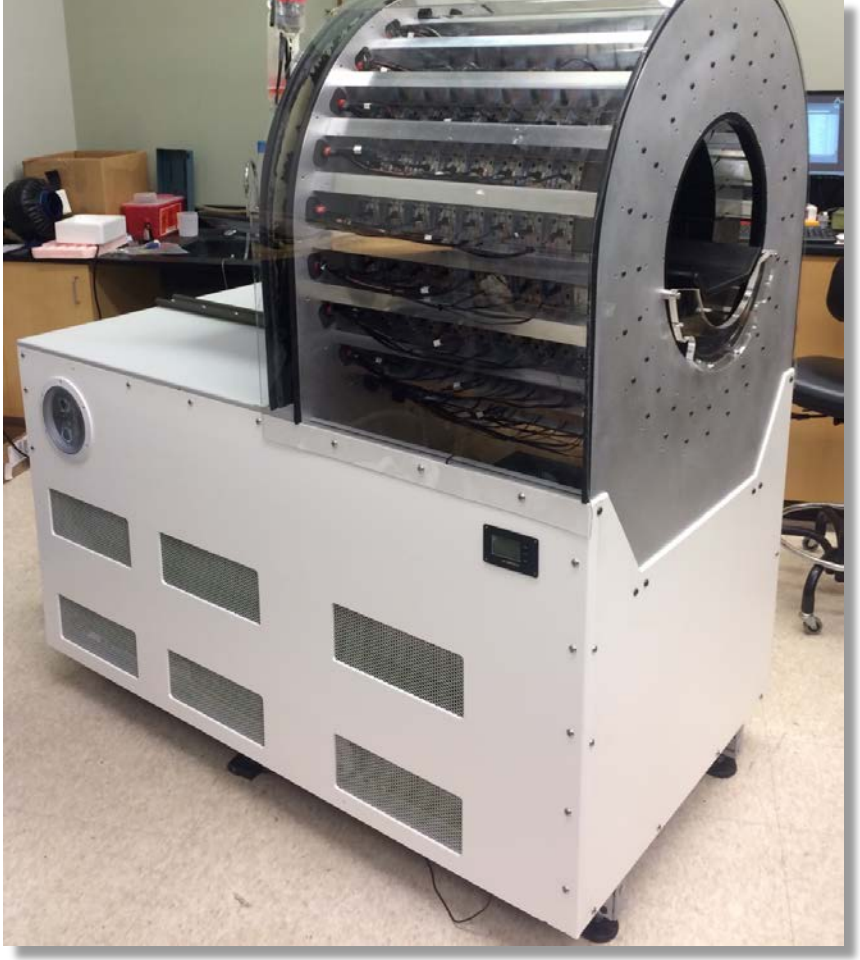

Constructed from the components of a prototype clinical scanner (Siemens mCT)

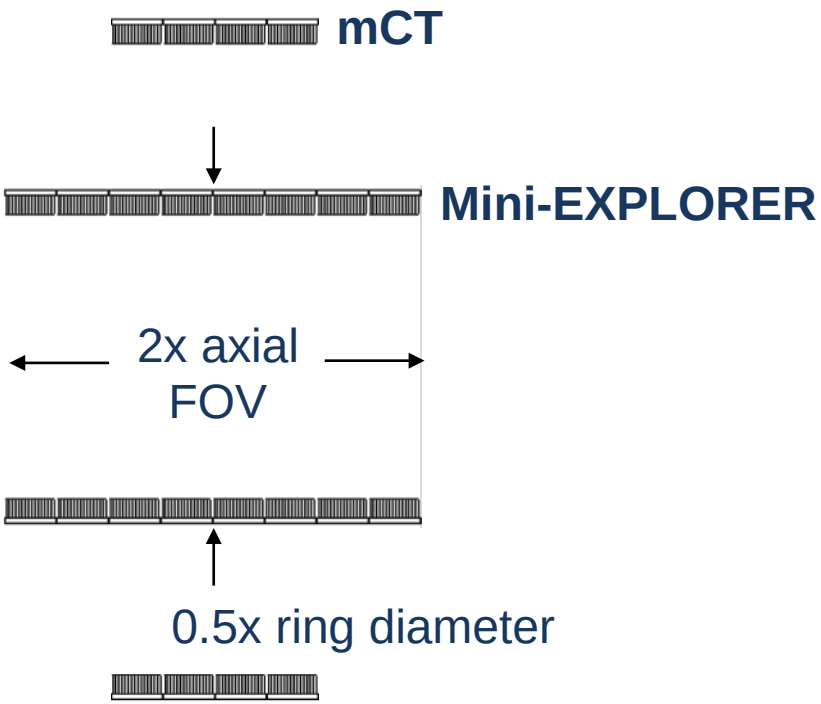

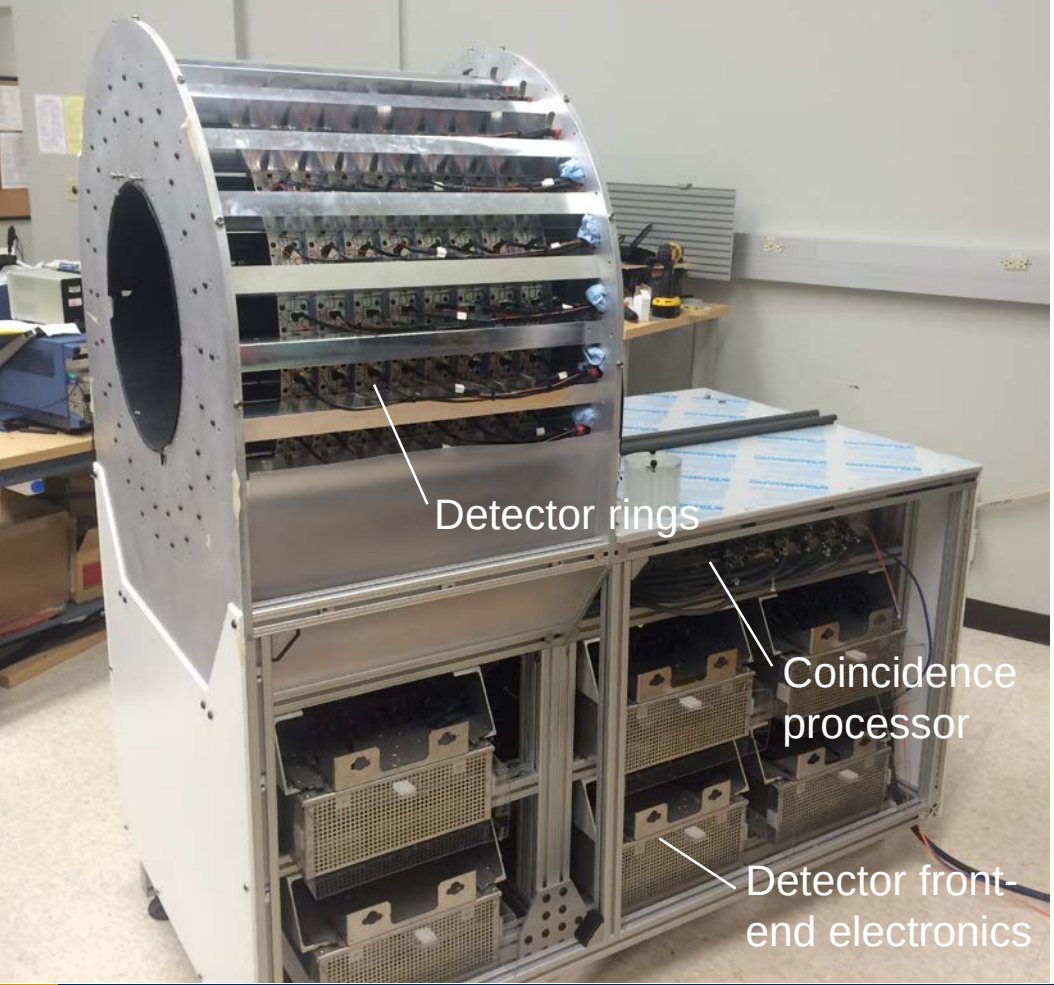

Scanner details

- 192 PMT block detectors
  - 13 x 13 array of LSO crystals (4 x 4 x 20 mm^3)

- Timing resolution = 609 +/- 3 ps

- No depth-of-interaction encoding

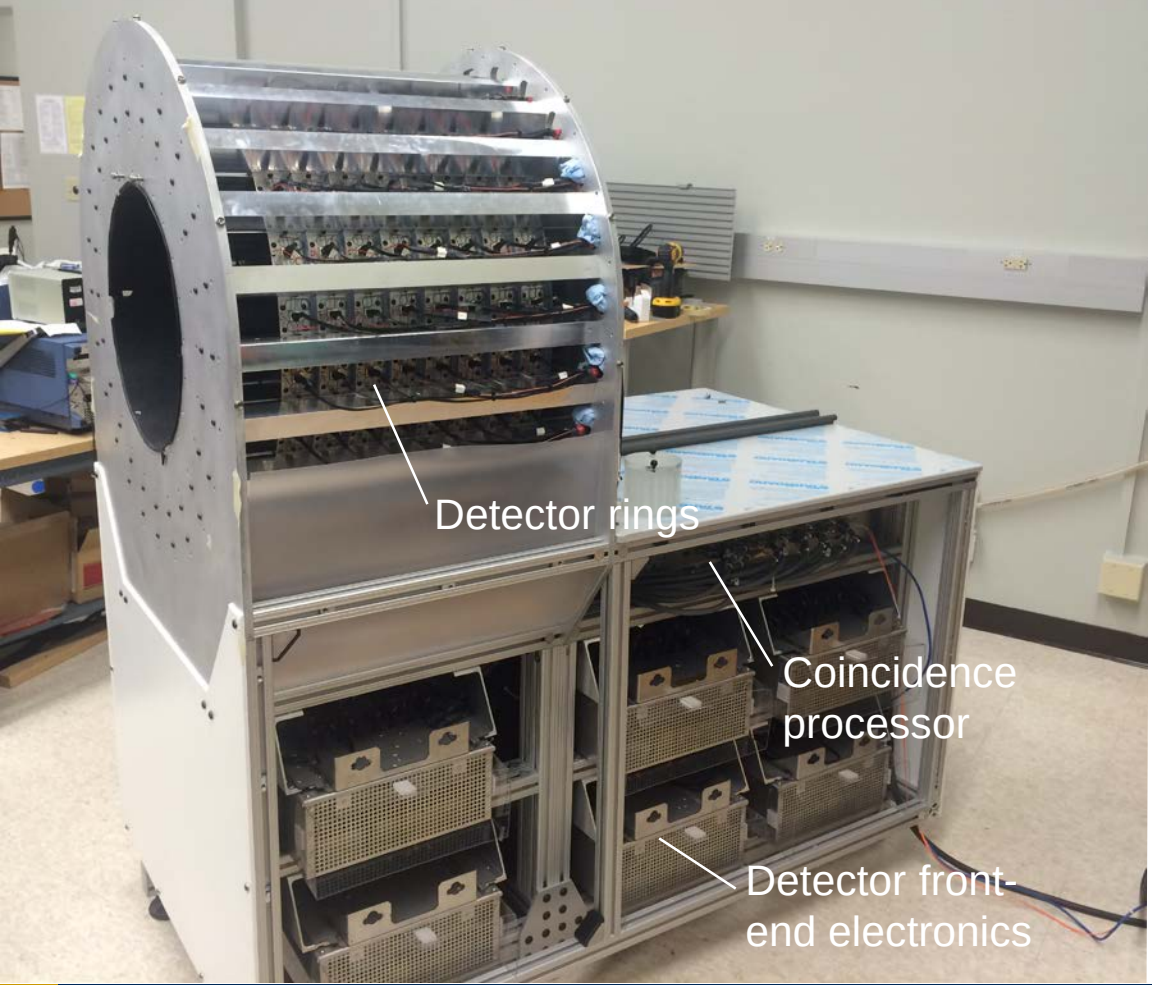
Detector rings
Coincidence processor
Detector front-end electronics

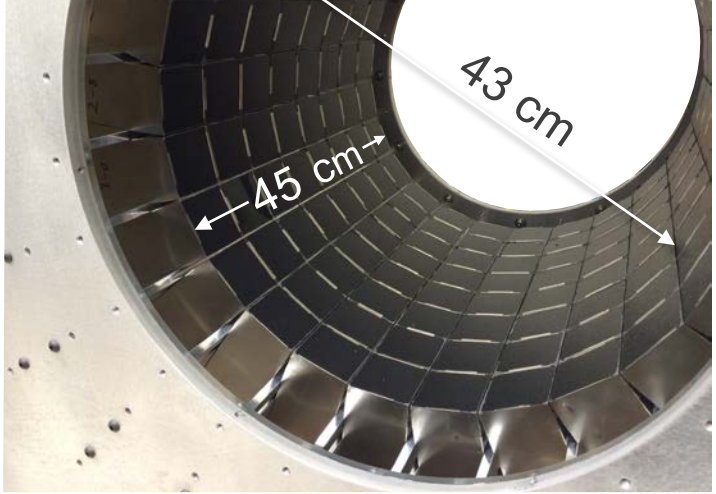
43 cm
45 cm

Experiment aims

1. Benchmark the scanner performance for monkey imaging.
2. What are the benefits / trade-offs of a wide acceptance angle?

Physical performance

- Sensitivity
- Noise equivalent count rate (NECR)
- Scatter fraction (SF)

Phantom imaging studies

- Image uniformity
- Transaxial spatial resolution
- Axial spatial resolution

Physical performance: methods

Measure physical performance over a range of acceptance angles

- Range of acceptance angles applied to listmode data in post-processing

- Coincidence time window determined for each event based on ring difference:

$$\tau = \frac{\sqrt{\left(FOV_{trans}\right)^2 + \left(\Delta z\right)^2}}{c} + 3\Delta t$$

(2.8 ns – 3.6 ns)

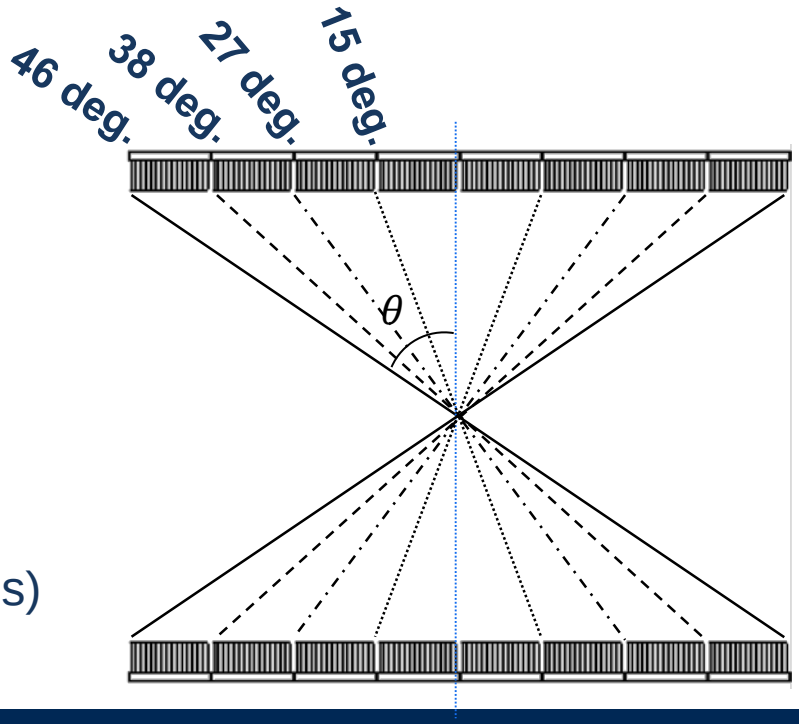

Sensitivity

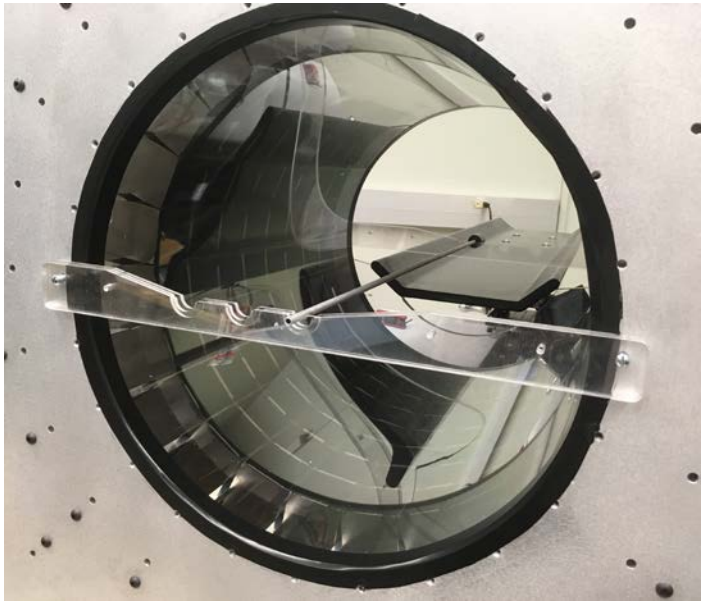

NEMA NU-2 sensitivity:

- 70 cm line source inside 1 – 5 aluminum sleeves
- 8 MBq ^{18}F-FDG
- Histogram listmode data into single slice re-binned (SSRB) sinograms for each acceptance angle
- Extrapolate sensitivity to zero aluminum thickness to compute scanner sensitivity

Sensitivity

Axial sensitivity (46 deg.)

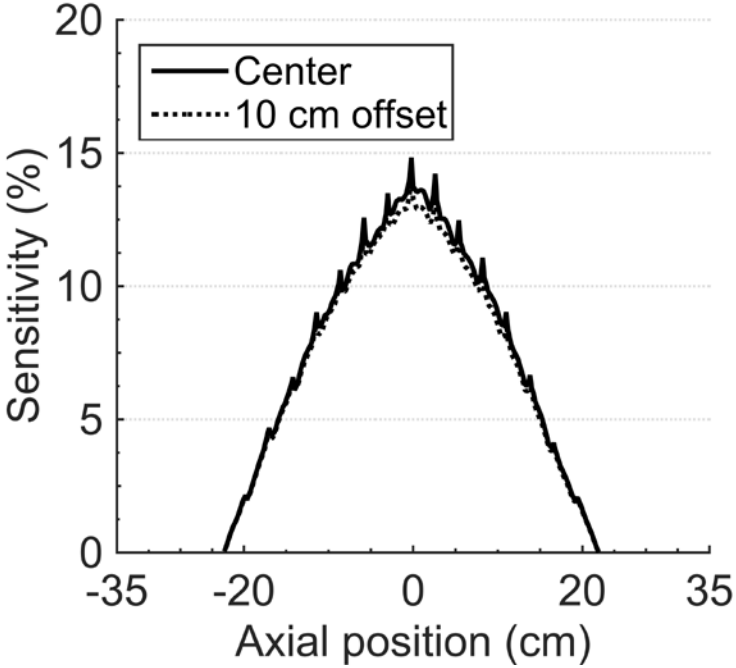

Total sensitivity vs. acceptance angle

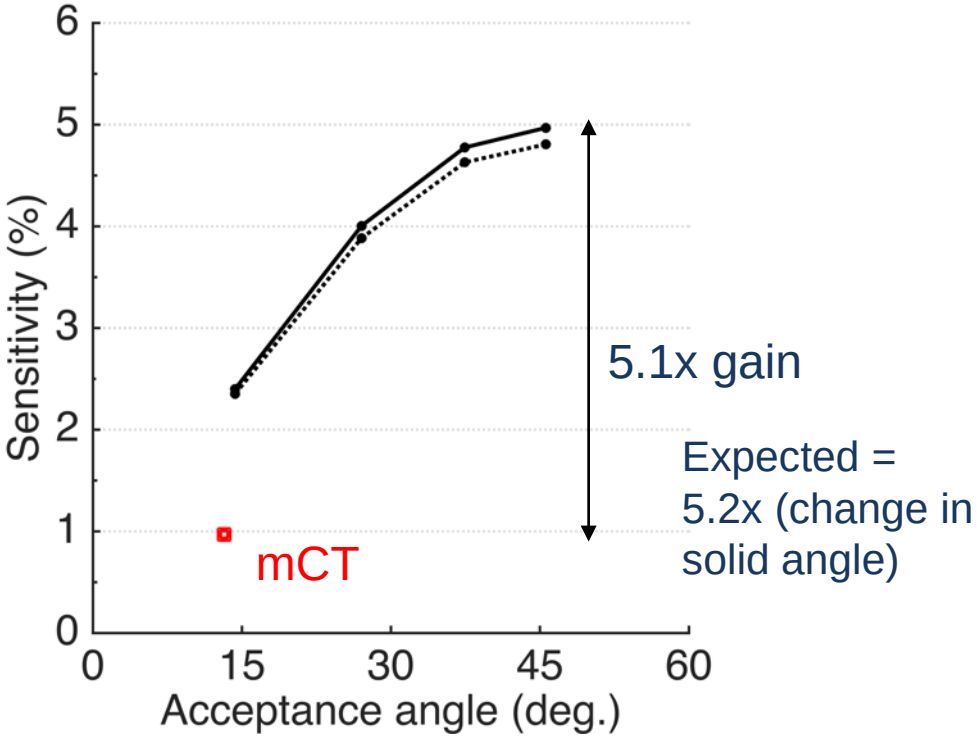

Noise equivalent count rate and scatter fraction

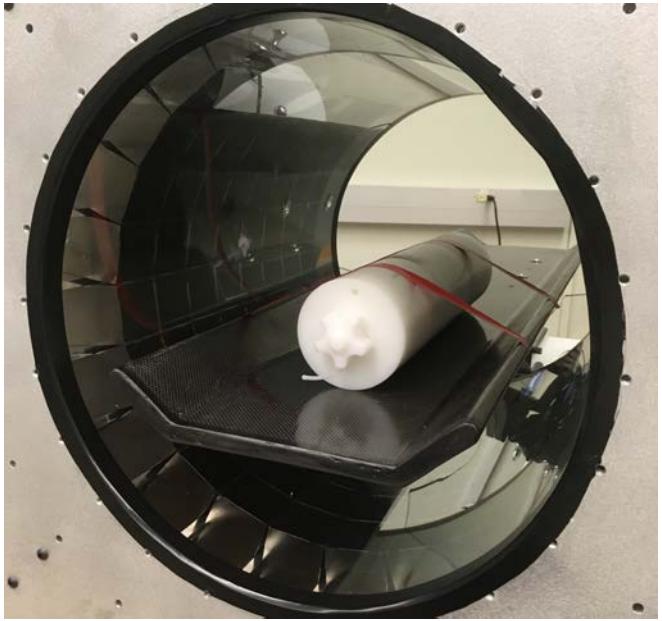

Monkey NU-4 scatter phantom

- 10 cm diameter
- 40 cm length

- 350 MBq ^{18}F-FDG

- Count rates (trues, scatters, randoms) extracted from SSRB sinograms for each acceptance angle (NEMA NU-4 2008 methods)

Noise equivalent count rate (NECR)

$$NECR = T\frac{T}{T+S+R}$$

Peak NECR

Acceptance angle (deg.)	*15*	*28*	*38*	*46*
NECR (kcps)	**895**	**1466**	**1707**	**1741**

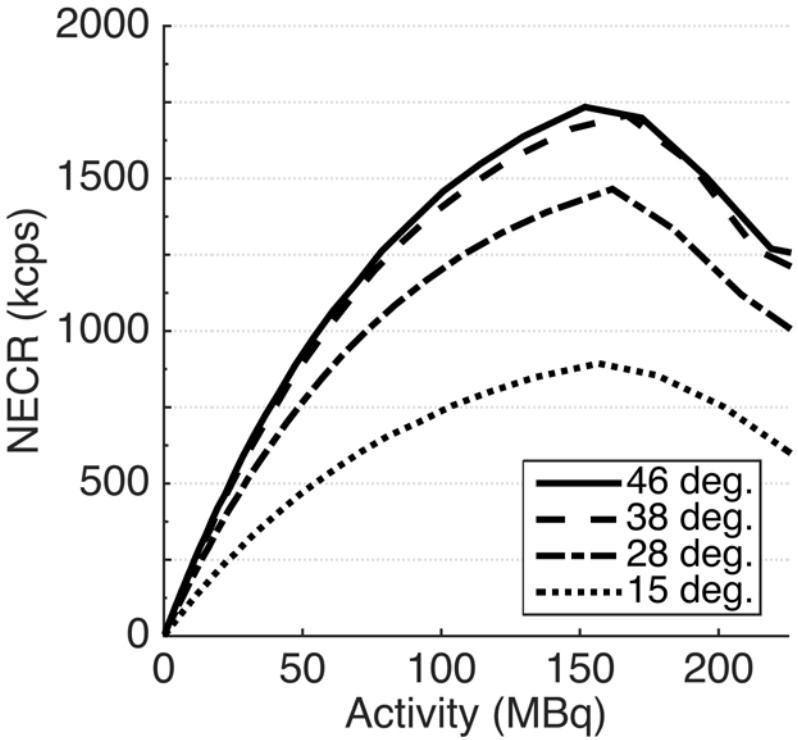

Scatter fraction

$$SF = \frac{S}{T + S}$$

Average SF up to peak NECR

Acceptance angle (deg.)	*15*	*28*	*38*	*46*
NECR (kcps)	**15.6**	**16.1**	**16.4**	**16.5**

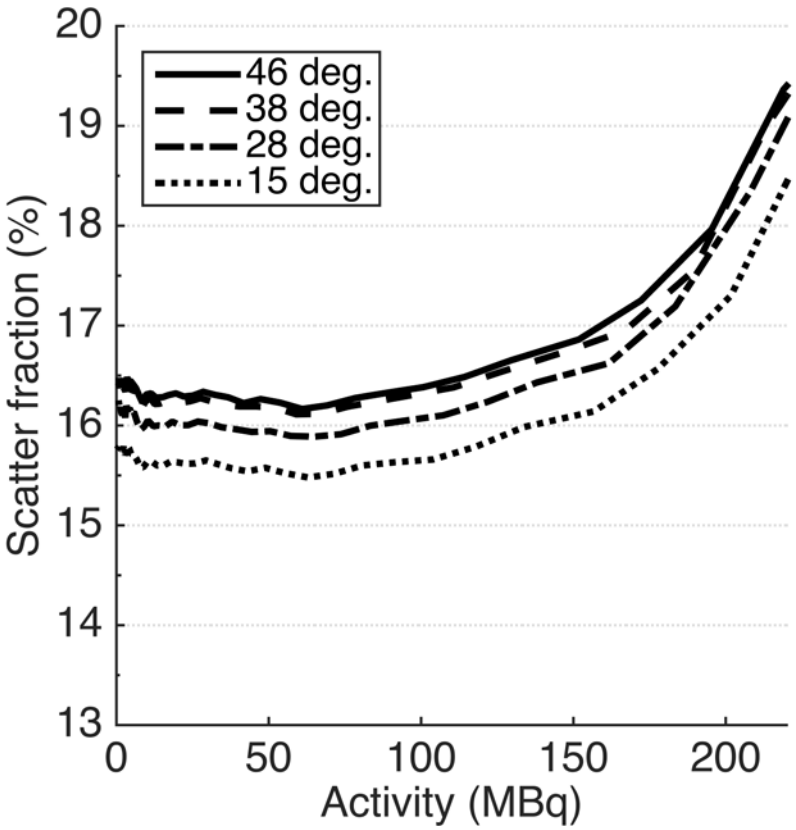

Phantom imaging

1) Uniform cylinder

Image uniformity
10 cm diameter, 50 cm length

2) Derenzo hot-rod

Transaxial spatial resolution
Rod diameter: 2 mm – 7 mm

3) Axial bars

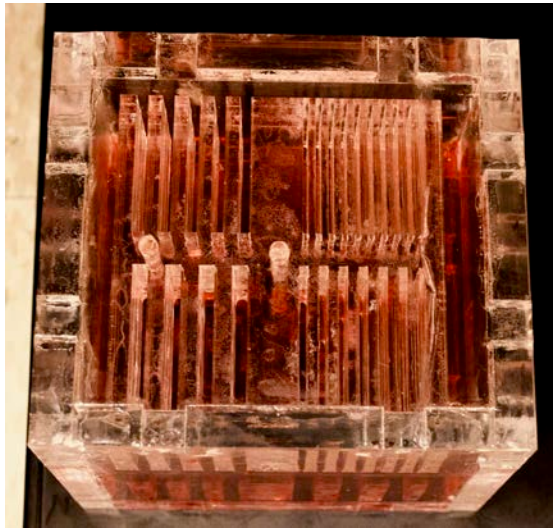

Axial spatial resolution
Bar widths: 2 mm – 9 mm

Image reconstruction

- **List-mode ordered subsets expectation maximization (LM-OSEM).**
- **Accurate resolution model in the system matrix (PSF modeling).**
- **Image voxel size: 0.5 x 0.5 x 2.0 mm^3.**
- **Time-of-flight (TOF) with 609 ps kernel FWHM.**
- **Corrections: Normalization and attenuation.**
  - Analytically derived μ-map for phantom images.
  - Currently no random and scatter correction.

Normalization

Concentric cylinder normalization phantom

- 4 mm OD (3 mm ID) tubing coiled around 30 cm diameter hollow acrylic cylinder.

- Iterative model-based algorithm to compute normalization factors[1].

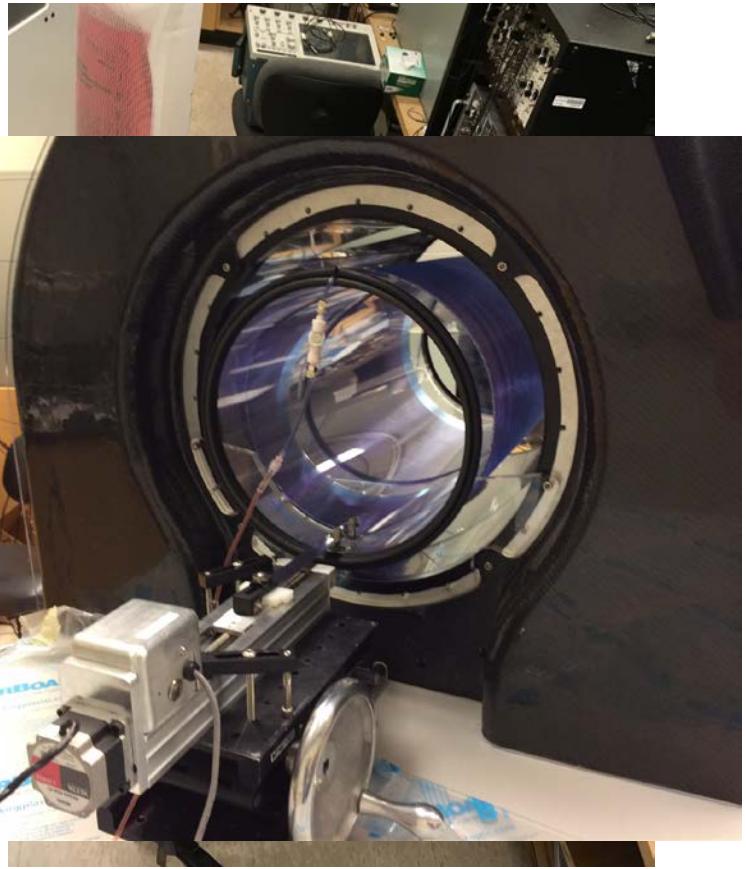

[1]Bai et al. Phys. Med. Biol. **47** pp. 2773, 2002

Image uniformity: Uniform cylinder images

- 46 degree acceptance angle
- 500 million events

Transaxial and axial uniformity

Transaxial variation: Radial line profile through average slice

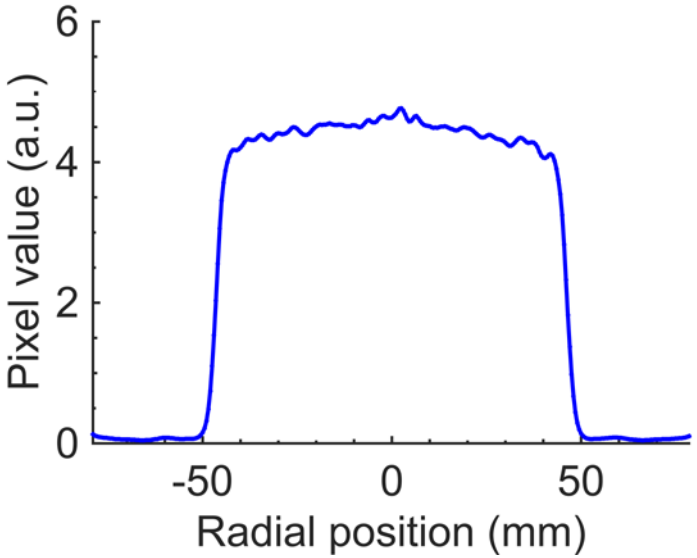

Axial variation: Average pixel value for each axial slice

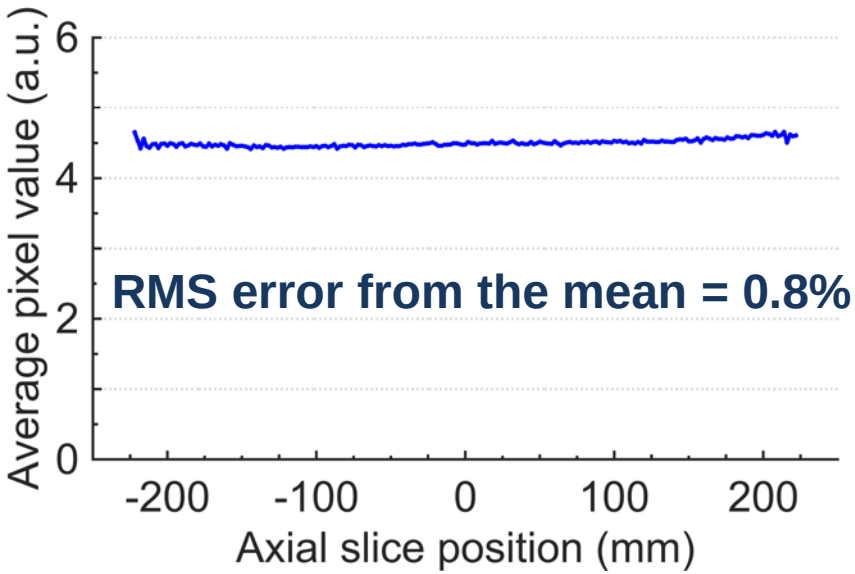

Derenzo hot-rod phantom

- 46 degree acceptance angle
- 400M events (10 min acquisition, 8 MBq ^{18}F-FDG)
- 3 iterations, 20 subsets

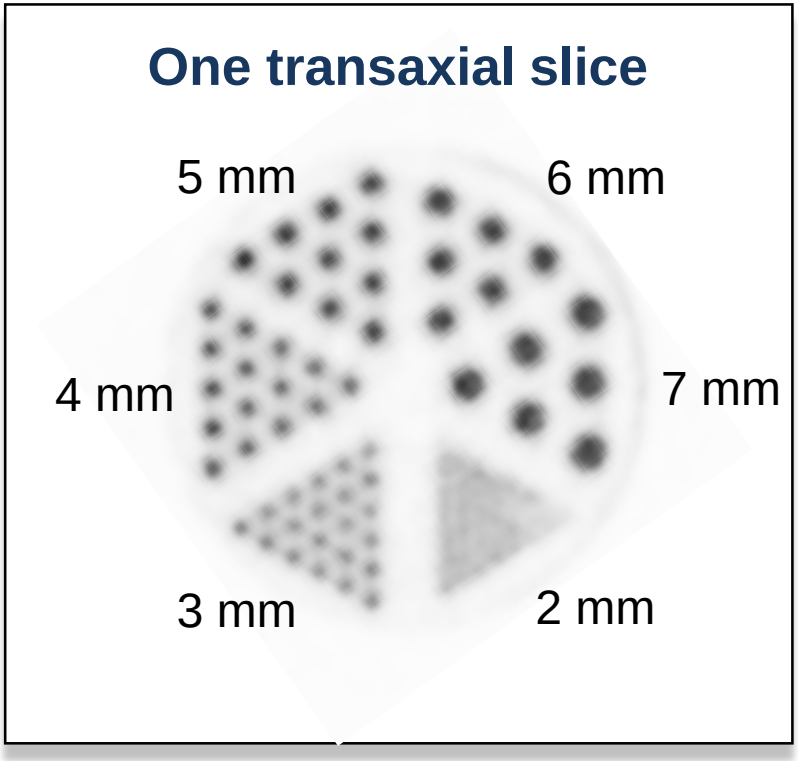

Axial spatial resolution: effect of acceptance angle

- 400M events for all acceptance angles
- 3 iterations, 20 subsets for all acceptance angles
- Quantify effect of acceptance angle by computing peak-to-valley ratio from line profiles

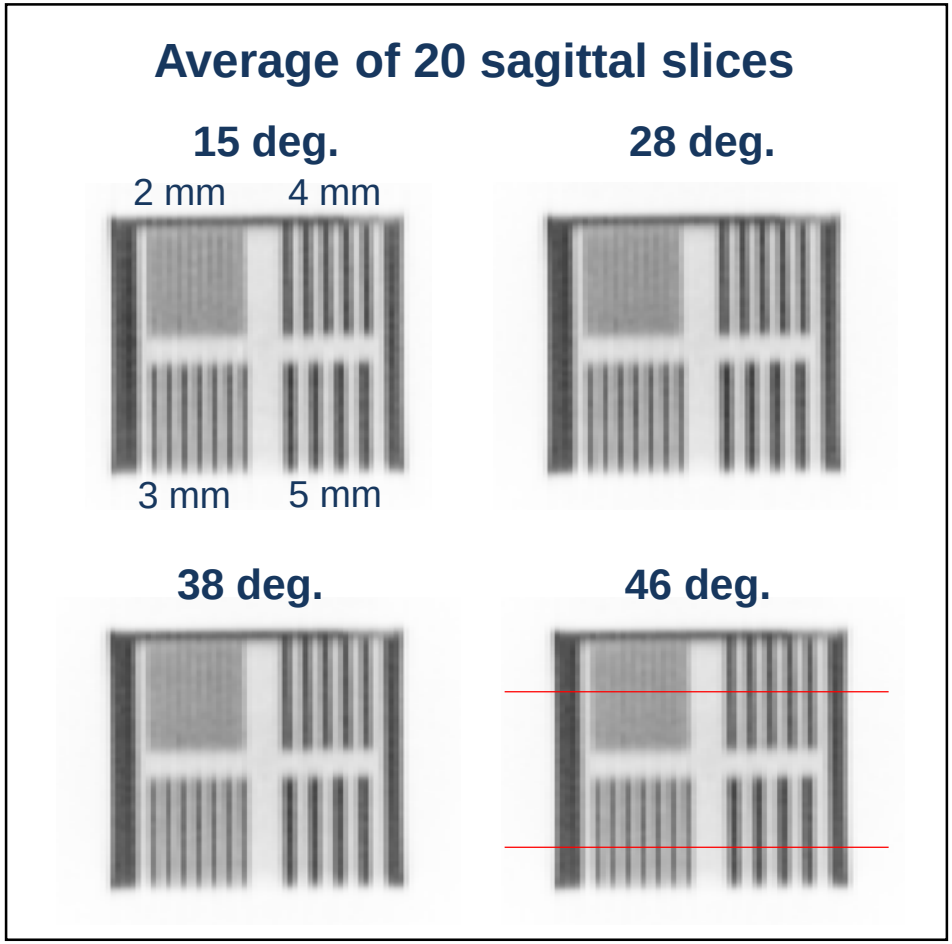

Axial peak-to-valley ratio

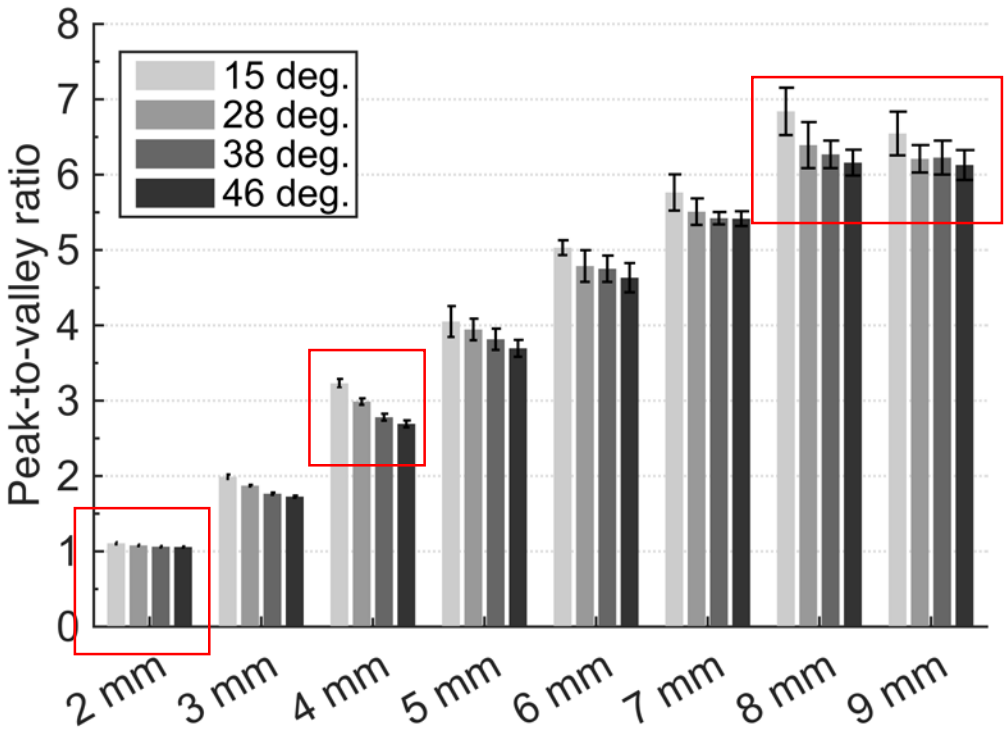

- **Small bar width:** p/v limited by partial volume and voxel width
- **Large bar width:** p/v converges to ~ 6 – 7
- **4 mm bar width:** maximum relative difference between 15 – 46 deg. acceptance angles (16%)

Conclusions

- **Sensitivity:** 5% total NU-2 sensitivity (5-fold higher than mCT), 15% peak
- **Count rate performance:** up to 1741 kcps peak NECR, 16.5% SF
- **Spatial resolution:** Resolve 3 mm structures transaxially and axially
- **Image quality:** Highly uniform image quality achieved with 46 deg.

Long axial FOV + wide acceptance angle provides high sensitivity with acceptable trade-offs for monkey imaging

Future work

Mini-EXPLORER is built and ready for imaging studies.

- Upcoming first animal study: canine imaging at UC Davis Vet. Med. before scanner is deployed at the Primate Center

- Investigate impact of wide acceptance angle, long axial FOV on image quality

- Implement all corrections for quantitative imaging

Acknowledgements

Funding: NIH R01 CA170874, UC Davis RISE, NSERC Postgraduate scholarship

EXPLORER team (explorer.ucdavis.edu)

UC DAVIS
UNIVERSITY OF CALIFORNIA

Ramsey Badawi
Simon Cherry
Jinyi Qi
Terry Jones

Julien Bec
Eric Berg
Martin Judenhofer
Edwin Leung
Emilie Roncali
Xuezhu Zhang

BERKELEY LAB

Bill Moses
Qiyu Peng

Penn

Joel Karp
Suleman Surti
Srilalan Krishnamoorthy